[HKK+18] S. Hillemacher, S. Kriebel, E. Kusmenko, M. Lorang, B. Rumpe, A. Sema, G. Strobl, M. von Wenckstern:
Model-Based Development of Self-Adaptive Autonomous Vehicles using the SMARDT Methodology.
In: Proceedings of the 6th International Conference on Model-Driven Engineering and Software Development (MODELSWARD'18), pg. 163-178. SciTePress, Jan. 2018.
www.se-rwth.de/publications

Model-Based Development of Self-Adaptive Autonomous Vehicles using the SMARDT Methodology

Steffen Hillemacher[1], Stefan Kriebel[2], Evgeny Kusmenko[1], Mike Lorang[1], Bernhard Rumpe[1], Albi Sema[1], Georg Strobl[2] and Michael von Wenckstern[1]

[1]*Software Engineering, RWTH Aachen University, Germany* http://www.se-rwth.de

[2]*BMW Group, Germany* https://www.bmwgroup.com

Keywords: Reference paper for SMARDT methodology in Automotive Industry, self-driving vehicles, modeling languages

Abstract: Cyber-physical systems are deeply intertwined with their corresponding environment through sensors and actuators. To avoid severe accidents with surrounding objects, testing the the behavior of such systems is crucial. Therefore, this paper presents the novel SMARDT (Specification Methodology Applicable to Requirements, Design, and Testing) approach to enable automated test generation based on the requirement specification and design models formalized in SysML. This paper presents and applies the novel SMARDT methodology to develop a self-adaptive software architecture dealing with controlling, planning, environment understanding, and parameter tuning. To formalize our architecture we employ a recently introduced homogeneous model-driven approach for component and connector languages integrating features indispensable in the cyber-physical systems domain. In a compelling case study we show the model driven design of a self-adaptive vehicle robot based on a modular and extensible architecture.

1 INTRODUCTION

In the exciting field of self-driving vehicles developers and researchers have been faced with a variety of interdisciplinary problems from areas such as control theory, electrical and mechanical engineering as well as computer science for many years (Urmson et al., 2008). Obviously, efficient development of autonomous driving systems is only possible by means of elaborated methodologies, languages, and tools providing a high level of automation (Baheti and Gill, 2011).

The complexity problem in automotive industry affects different phases and elements of system development, especially the specification of the requirements, the design and the architecture of the systems as well as their integration and testing (Grimm, 2003). Right now, the V-Model approach is used to create requirements and informal design as well as specification or functionality models on the left side for the system in different abstraction layers. Each layer on the left side has a corresponding testing step on the right side in the V-Model. But the development and maintenance (e.g. due to feature evolution) of these tests are done manually most of the time. This leads to several disadvantages: (1) the test model on the right side may become inconsistent to its original specification on the left side, (2) updating the specification requires an update of all handwritten tests this specification links to, (3) due to time pressure, often only the functionality on the lower layers is updated, whereas requirements and design specification of the layers above become inconsistent with the updated behavior, which may lead to misunderstandings inside the team and make the documentation obsolete, (4) the SysML specification is so general (Liang et al., 2004) that different teams in a company may interpret or understand these diagrams semantically differently.

To overcome all of these shortcomings, the SMARDT approach (Specification Methodology Applicable to Requirements, Design, and Testing) uses only a strict and formalized subset of SysML diagrams so that for each layer test cases can be derived automatically to test whether the developed system satisfies the specification of each layer. This enables higher consistency between different abstraction layers of the V-Model when using an agile development process.

This reference paper introduces the novel SMARDT methodology with its focus on algorithms for deriving test cases from activity diagrams and (internal) block diagrams that are used to model the system behavior in the different abstraction layers. All presented diagram types to

model software in the different layers are explained in a case study showing the model-based design of a self-adaptive autonomous racing car tuning its control parameters after each lap in order to improve its driving behavior.

Component & Connector (C&C) architectures have proven to be an appropriate approach for the domain opening up a data-flow driven and hierarchical perspective on the system. Prominent examples of C&C languages originating from the control domain are MATLAB Simulink (Mathworks Inc., 2016), Modelica (Modelica Association, 2005; Elmqvist et al., 1999), AutoFocus3 (Aravantinos et al., 2015), LabView (National Instruments, 1998), Verilog (Accellera SYSTEMS INITIATIVE, 2014), VHDL (The Institute of Electrical and Electronics Engineers, 1988; Ashenden, 2010), JigCell (Palmisano et al., 2015), and Scade (Dormoy, 2008). They support the system designer with a broad set of libraries, a discrete time simulator, as well as efficient code generation for different targets. However, Cyber-Physical System (CPS) developers can find themselves confronted with a series of drawbacks when using modern C&C languages such as the lack of a unit based type systems, missing component and connector reuse concepts, as well as an overwhelming user interface. A comparison of state-of-the-art C&C languages and their shortcomings with the focus on the CPS domain was given in (Kusmenko et al., 2017). Furthermore, an integrated and homogeneous model-driven framework named MontiCAR was introduced addressing these issues.

This paper evaluates MontiCAR inside the SMARDT process to show how MontiCAR overcomes the identified difficulties of C&C languages. As our target we choose OpenDaVINCI, a middleware which has proven to be an efficient basis for automated driving applications in recent years (Berger, 2016). This allows us to generate distributed and realtime-capable architectures. We then evaluate and test our models in the widely used Open Racing Car Simulator (TORCS).

The contribution of this paper are the following: (1) We present a development process for embedded systems which is conform with ISO 26262. This process consist of four layers: object of reflection (textual requirements and use cases), logical layer (functionality modeled by abstract C&C models and underspecified activity diagrams), technical concept (deterministic C&C models and C-code), and realization (e.g., ECUs, CAN-BUS, Flexray, and timing). (2) We evaluate MontiCAR as a formal and stream based C&C modeling language for CPS behavior specification. (3) We present an algorithm which is capable of creating a realization model from the concrete technical concept by binding all configuration parameters. An evolutionary algorithm is used. (4) Finally, in a compelling case study we show the design of a self-adaptive vehicle robot based on a modular and extensible architecture.

The remainder of the paper is structured as follows: first, a running example is presented in Sec. 2 in order to make the reader familiar with the difficulties arising when developing CPS. Thereafter, Sec. 3 shows the first main contribution, the SMARDT approach. The second layer of SMARDT is discussed in Sec. 4. In Sec. 5 the models of the third SMARDT layer are presented in more detail. Next, Sec. 6 shows how input and output streams for functional testing of C&C models are generated. The experiments conducted in Sec. 7 underline the feasibility of the SMARDT methodology. Finally, we conclude our paper in Sec. 8.

2 RUNNING EXAMPLE

On the physical side, one of the main differences of an autonomous vehicle compared to a manned one is the enormous variety of sensors the automated vehicle needs to be equipped with. These sensors are required to perceive the environment as accurately as possible. For example, a GPS receiver senses satellite signals in order to recover its own position, ultra-sonic transducers can localize obstacles by measuring ultrasound echoes. Complex detection and understanding of objects and their relationships can be done using cameras and computer vision techniques. On the other hand, the actuators provide a means to manipulate the physical state of the vehicle by (1) accelerating, (2) braking, and (3) steering. The behavior of the vehicle can now be defined as a computational model mapping the vehicle's goal, its sensor inputs, as well as other accessible knowledge such as maps to actuator commands. Ideally, the software developer would not need to know the technical manufacturer specific details of the sensors and actuators installed in the vehicle but would rather get a homogeneous access to all available sensor and actuator data via a common interface. As a running example for the further development we will develop a self-driving racing car system. Such a vehicle needs to have a precise steering even for high velocities. On the other hand, no complex urban situation understanding and decision making is necessary allowing us to concentrate on the development of the controller system. We model our self-driving vehicle as a cuboid of length L, width W and height H. We assume that the vehicle has full ac-

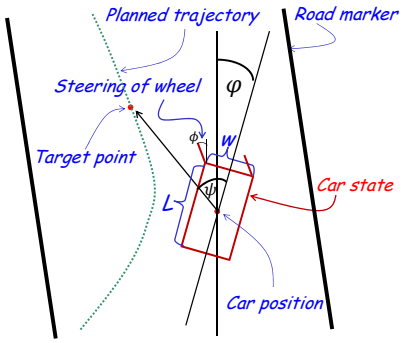

Fig. 1: Sketch of the vehicle and main quantities.

cess to the map of the track it is driving on. Furthermore we assume, that it possesses a series of sensors measuring the speed v, wheel angle ϕ , the position of the car x as well as its yaw φ up to a certain precision as depicted in Fig. 1. Usually, the behavior of an autonomous control system is defined not only by the algorithm or the model but also by a well chosen set of parameters θ. Often, the optimal parameter set varies from one physical vehicle realization to another due to differences in configuration, software evolution but also random physical factors introduced during manufacturing and may even change during the lifetime of a CPS. Since fine tuning these parameters for every single vehicle is infeasible due to the high cost, the vehicle should detect and re-adjust its operating point on-line.

3 SMARDT METHODOLOGY

With the introduction of ISO 26262, an international standard for functional safety of road vehicles, the demand for a new specification methodology for safety-relevant automotive functions arose. As a result, the *Specification Methodology Applicable to Requirements, Design, and Testing (SMARDT)*[1] was developed. SMARDT is based on the German V-Model (Bröhl and Dröschel, 1995), the official project management methodology of the German government.

In the basic V-Model the left side represents the decomposition of requirements and creation of system specifications. The right side, on the other hand, represents the integration of developed system parts and their validation. In general, the V-Model structures requirements and specifications of a system in different abstraction layers. Each layer on the left side has a corresponding testing step on the right side.

[1]The original abbreviation SMArDT is related to the German term "**S**pezifikations-**M**ethode für **A**nfo**r**derung, **D**esign und **T**est"

However, the creation of these tests is done manually most of the time. This leads to several disadvantages:

- Ensuring consistency between the tests on the right side and the specifications on the left side becomes difficult, since only vague links between tests and specifications exist.
- Updating the specifications results in the necessity of a manual update of all the corresponding handwritten tests.
- Extending a system's functionality is mostly done only on the lowest layer due to time pressure. Requirements and specifications of the higher layers, however, are not updated accordingly.

To overcome all of these shortcomings, the SMARDT approach uses only a strict and formalized subset of SysML diagrams (OMG, 2015) with a meaningful and clear semantics (Harel and Rumpe, 2004) to specify the functionality of a system. As a consequence, a higher consistency between different abstraction layers of the V-Model is achieved, especially for agile development processes, which are mostly iterative, incremental, and evolutionary (Beck et al., 2001). The rigorous mathematical theory behind the used SysML diagrams enables further validations such as (1) backward compatibility checks (Rumpe et al., 2015; Richenhagen et al., 2016; Bertram et al., 2016) for software maintenance and evolution between different diagram versions of the same layer as well as (2) refinement checks (Rumpe, 1996) between diagrams of different layers for detecting inconsistencies in specifications between different layers, mostly between the first and second one. This paper's main focus lies on the testing part of the SMARDT approach to enable agile modeling (Rumpe, 2017) in SysML.

In general, SMARDT describes a formal specification for requirements, design, and testing of system engineering artifacts according to the ISO 26262 specifications, as illustrated in Fig. 2. Four abstraction layers structure the method:

1. The first layer contains a first description of the object under consideration and shows its boundaries from a customers point of view.
2. The second layer contains functional specifications without details of their technical realizations.
3. The third layer embraces the technical concepts of the system.
4. The fourth layer represents the software and hardware artifacts present in the system's implementation.

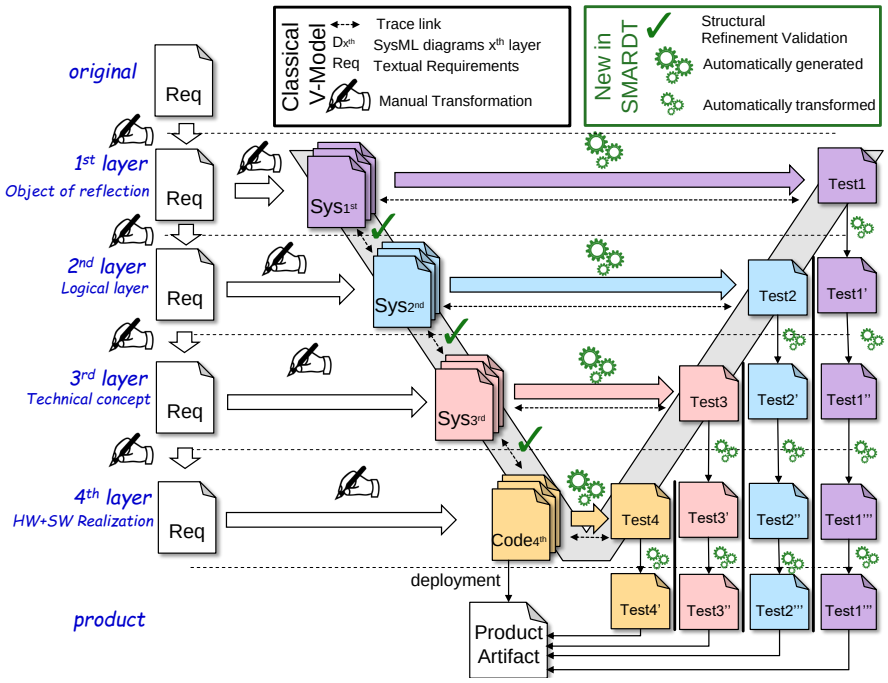

Fig. 2: Overview of the SMARDT methodology.

As depicted by Fig. 2, SMARDT achieves a higher consistency between the different layers by verifying and model-based testing (Philipps et al., 2003) that the final product meets the requirements of all layers. More specifically, SMARDT enables structural verification as discussed in (Bertram et al., 2017) between each layer indicated by the green check marks in Fig. 2. Furthermore, SMARDT enables a systematic and fully automatic derivation of test cases for each layer by allowing only a formalized subset of SysML diagrams on each layer (Rumpe, 2003). Finally, SMARDT ensures consistency between the test cases of each layer by enforcing that the test cases of one layer can also be used on the lower layers by transforming them. This is illustrated on the right side of Fig. 2. For instance, layer 1 describes functionality of the product on the highest level. Hence, the corresponding test cases cannot be used directly on the lower layers, and therefore must be transformed to multiple low-level test cases (Pretschner et al., 2004). This is done, for instance, by substituting abstract signal names and values with concrete hardware signals and values.

The first two abstraction layers are conceptual in the sense that their diagrams lack a direct counterpart in the implementation. The behavior modeled within the diagrams can later be implemented across several components. Moreover, signals used in these diagrams are logical, i.e., they abstract away from signals of the implementation. Consequently, corresponding values comprise a range of values present in the implementation. In contrast, the elements of the third and fourth layers have a direct representation within the implementation. The third layer describes hardware-independent functionality of a system, whereas the fourth layer contains software parts that are specific to a given micro-controller and also handles low-level behavior such as I/O-interrupts.

A lot of research about improving and tailoring the V-Model to company-specific needs at management level has been conducted (V-Modell XT, 2006; Broy and Rausch, 2005; Friedrich et al., 2009). In contrast to these works, the SMARDT methodology focuses not on integrating the process into different business structures but rather on the formal and technical parts of the specification diagrams of the different layers in the V-Model to have a traceable, verifiable, consistent, and particularly, testable artifacts over the entire development process.

The rest of this paper applies the SMARDT methodology for developing a self-adaptive autonomous vehicle. Fig. 3 shows how the original requirement of a *superior driving experience* is stepwise refined to concrete technical ones. Each layer refines the requirements of the higher layers by adding more details. Starting with the original requirement **R1**, each layer subdivides this requirement into more specific ones. Consequently, SMARDT enables tracing the requirements through all layer. Moreover, Layer 3 is divided into 3A (generic technical concept)

and 3B (concrete technical concept). The generic technical concept presents a functional architecture with unbound configuration parameters, while in contrast the concrete technical concept binds all the configuration parameters. In this way the architecture of layer 3A can be reused in different model series. Different car engines, dimensions, weights, and wheelbases but also variations in the manufacturing process are reasons why cars expose different behaviors in their environment. Hence, no general controller exists and car-specific parameters must be derived in Layer 3B.

4 ACTIVITY DIAGRAMS FOR SMARDT LAYER 2

We present a version of SysML activity diagrams exhibiting formal expressions (Maoz et al., 2011). Using these expressions we are able to provide detailed specifications of the functionality modeled on the second layer of SMARDT. Although these high level specifications are independent of the technical concept, they still can be used to describe abstract system constraints without predetermining the way they have to be implemented.

For formal expressions we use the OCL/P specification language (Rumpe, 2016), which is a Java-based OCL derivate. OCL is well suited for implementation-independent high level specifications describing system constraints (Gogolla et al., 2007). Another benefit of OCL/P is its extension for units (Maoz et al., 2017), making it even more suited for embedded systems.

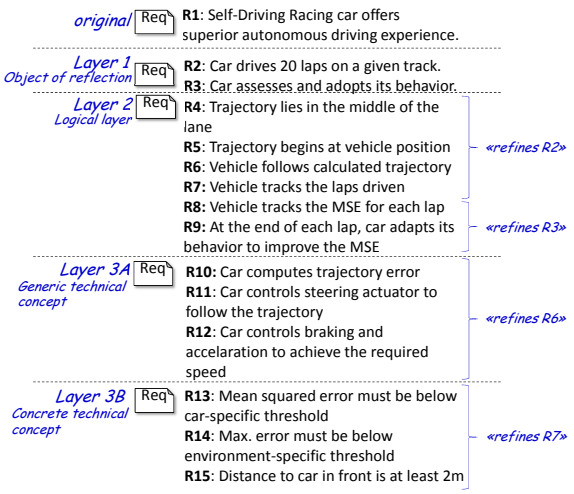

Fig. 3: Requirement refinement in a simplified SMARDT process.

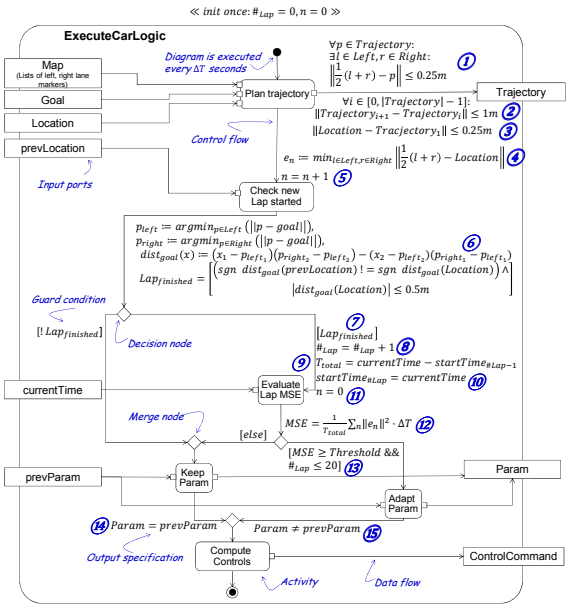

Fig. 4: Activity diagram describing the car logic executed in each time step.

Example Activity Diagram To show how OCL/P is used, Fig. 4 illustrates a simplified activity diagram (AD) describing the car logic. In general, the structure of the ADs used on the second layer of SMARDT is similar to the SysML standard. Inputs and outputs of the function are modeled using ports. Besides the control flow, the object flow of a diagram explicitly indicates when and where the information is passed. Action nodes are used to model single steps of the function. Control nodes, e.g., decision nodes, model any decision logic and parallelism of a function. For the description of the former we added OCL/P expressions to the diagrams. As These expressions are used as guards, but also to extend the control flow edges. Without loss of generality and for better readability we use pure mathematical expressions for the formal specification in Fig. 4. However, this notation can easily be translated to OCL/P as will be shown in the following. This way, each edge not only models the control flow of an AD, but can also be used to build up an OCL/P expression. For instance, the outgoing edge of the action `Check new lap started` contains a formal expression providing several definitions and an assignment. The newly assigned $Lap_{finished}$ is used in the guards of the following decision node. Depending on its evaluation different actions are performed next.

As the example AD of Fig. 4 demonstrates, by extending ADs with formal logics we are able to model powerful formal expressions within a diagram. These expression can be used as high level specifications to describe abstract system constraints as well as a basis

for automated test case derivation.

As is common for embedded systems, the designed software of our example is executed in three phases: (1) the initialization phase, (2) the main loop, and (3) the exit phase. At system initialization the lap and cycle counters are set to zero. In the main loop the activity diagram is executed in every time step thereby exhibiting the following behavior. First, the trajectory is computed based on the abstract map (represented by two lists of left and right lane markers, respectively), the vehicle's goal, and its current location. Thereby, the resulting trajectory has to fulfill the following constraints:

- ① The trajectory does not deviate by more than 0.25m from the road middle line which can be formalized in OCL/P as `forall p in Trajectory: exists l in Left, r in Right: norm(0.5*(l+r)-p)<= 0.25m`.
- ② The discrete trajectory consists of points, which are at most 0.5m apart: `forall i in 1 .. Trajectory.size - 1: norm(Trajectory[i+1] - Trajectory[i]) <= 1m`.
- ③ The first trajectory point is within a radius of 0.25m from the current car position: `norm(Location - Trajectory[1]) <= 0.25m`.

Apparently, OCL/P is close to the pure mathematical notation provided in Fig. 4. Once the trajectory is computed, ④ the error which is defined as the distance between the car and the road middle line is computed for later evaluation and ⑤ the cycle counter is incremented. The car checks whether it just started a new lap by ⑥ analyzing if it crossed the line between the left and right road markers closest to the goal. If ⑦ a new lap is started, ⑧ the lap counter is incremented, ⑨ the total lap time for the finished lap is computed, ⑩ the start time of the new lap is set, and ⑪ the cycle counter is reset. Then ⑫ the mean squared error (MSE) for the finished lap is computed. If ⑬ the MSE is above a specified threshold and the car has not finished a total of 20 laps, the parameters are adapted and ⑮ must differ from the old ones. Otherwise the old parameter set is kept ⑭. Finally, the control commands are computed and outputted terminating the execution cycle.

It is also possible to specify well-formedness rules (such as stability, smoothness, and responsiveness (Matinnejad et al., 2017; Slicker and Loh, 1996)) for the output ports (e.g. ControlCommands) of closed-loop-control systems. An example of a smoothness rule specified in OCL/P could be that the difference of two successive steering control commands should be smaller than two degrees.

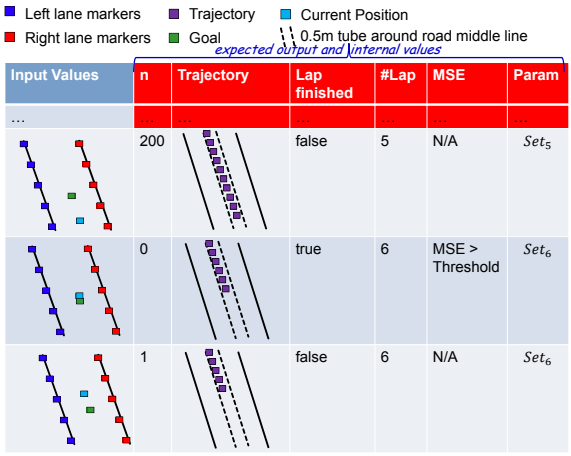

Fig. 5: Exemplary test case derived from the AD in Fig. 4.

Deriving Test Cases from Activity Diagrams Besides providing high level specifications, introducing formal OCL/P expressions to activity diagrams (ADs) also enables a systematic derivation (Mingsong et al., 2006) of test cases. The output of the derivation process are test cases, which can be used to test the functional specifications modeled by the ADs.

The basic approach for the derivation of test cases consists of several steps. First, the interface of the AD, respectively the modeled function, is determined. This can easily be done, since inputs and outputs are modeled explicitly in the AD by ports. Second, the set of paths through the diagram fulfilling the path coverage criterion *C2c* (Liggesmeyer, 2009), with each loop iterated once, is calculated. Based on this set, for each path a formal expression is built. This is done by analyzing each edge of the path and extracting the OCL/P expression. Third, for a set of initial conditions, the AD can be executed an arbitrary number of times and depending on the current input values the expected output and internal values can be calculated. During the calculation, the OCL/P expression of the specific path through the AD is evaluated. In the end, the resulting test case consists of a sequence of evaluated execution cycles.

Fig. 5 presents an excerpt of an exemplary test case in form of a table derived from the AD shown in Fig. 4. The excerpt shows a test sequence between lap 5 and 6. Each row represents one execution of the AD. For better readability the input values as well as the trajectory are presented graphically instead of concrete values. For the input values differently colored markers are used depicting the map, i.e., left lane and right lane, the current position of the car, and the goal. The expected output and internal values are to the right of the column containing the input values. The expected output and internal values include, for

instance, the current lap and parameter set of the respective diagram execution. Given the input values of each execution, the expected values are calculated by evaluating the OCL/P expression of the path through the diagram.

The derived test cases for the ADs of SMARDT layer 2 can be transformed to test cases for the following layers. Note that since the ADs of layer 2 only model the functional specifications without details of their technical realizations, the abstract signal names used in the ADs need to be mapped to the concrete technical signals used on the lower layers. As shown in Fig. 2 test cases for layer 3, layer 4, and the final product are generated based on the activity diagram. The test cases of layer 3 allow early detection of functional errors to avoid inconsistencies as early as possible. While the test cases for layer 4 ensure that the Hardware/Software integration did not introduce any functional incorrectness (e.g. variable overflow), the test cases for the final product ensure that the customer experience is as it is described in the activity diagram.

5 COMPONENT AND CONNECTOR MODELS FOR SMARDT LAYER 3

Existing Approaches to Model Self-Driving Cars Self-driving vehicle architectures have been discussed in several works. In (Montemerlo et al., 2008) a modular architecture which proved to be successful in the DARPA urban challenge was proposed. It consists of four layers, namely, the sensor interface, perception, navigation, and a user / vehicle interface. A series of heterogeneous sensors enable the vehicle to perceive its environment. A similar approach dividing the architecture into perception, behavior and planning is presented in (Wei et al., 2013). It enables the vehicle to cope with different kinds of situations by allowing to integrate a variety of intelligent behaviors. A common issue with the presented architectures are high sensor costs. This issue has been addressed, e.g., by Daimler in the Autonomous Bertha project (Ziegler et al., 2014) where a cheaper computer vision based approach was evaluated. Deep learning approaches have been emerging in the last years, trying to mimic a human driver by learning from image examples, i.e., only requiring camera inputs. In the end-to-end learning approach, the network tries to predict the best actuator commands directly after seeing the image (Bojarski et al., 2016). On the other hand, the goal of the direct perception architecture discussed in (Chen et al., 2015) is to let a neural network extract features such as distance to the front car from an input image. Then, the predicted feature set is passed to a conventional controller in order to generate actuator inputs.

In the domain of control Simulink (Mathworks Inc., 2016) is one of the dominating C&C frameworks. Simulink lacks a unit based type system but provides a variety of static analysis features, matrix support, and a large component library. Further relevant C&C languages, often specialized to a particular domain include LabView (test, measurement and control domain) (National Instruments, 1998), SysML (systems engineering domain) (OMG, 2015), VHDL (integrated circuit domain) (The Institute of Electrical and Electronics Engineers, 1988), Modelica (Modelica Association, 2005) and others. A detailed overview and comparison is given in (Kusmenko et al., 2017).

Overall Architecture An overview of the scenario we are going to develop in this section is depicted in Fig. 6. The plant we are using to evaluate our system is a TORCS vehicle residing inside the simulator on the left hand side of the figure. The actual self-driving functionality resides in the driving module including sensor signal filtering, trajectory planning, as well as a closed loop controller aiming to fulfill the vehicle's goal as efficiently as possible.

The data adapter provides an interface to read sensor data from the vehicle and write actuator commands thereby decoupling the self-driving software from the physical vehicle platform. By means of the filtered sensor data and the trajectory planing component, the controller computes the actuating values which are then sent through the data adapter back to the vehicle in the simulation.

Often it is necessary to experimentally evaluate different variants and configurations of a system to find the optimal solution for a given task. Therefore, modularity and loose coupling are essential in the development of CPS. However, a correct structural model of the controller is neither sufficient to guarantee a correct behavior of the system nor an appropriate parametrization thereof. As an example, our controller architecture is based on the classical and well-studied PID controller the basic behavior of which can be defined in parallel form as

$$y(t) = Pe(t) + I\int_0^t e(\tau)\,d\tau + D\frac{\partial e}{\partial t}. \qquad (1)$$

Now, each PID controller instance requires a set of at least three configuration parameters from a continuous search space. Finding a working set of parameters for a system consisting of a series of PID controllers and other parameterizable components by a

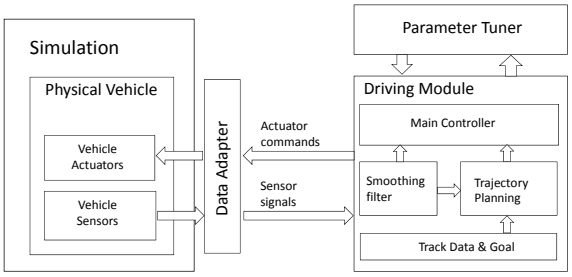

Fig. 6: Overall Architecture

brute force search is therefore infeasible. Thus, an intelligent approach to automate the tuning of the PID parameters is needed. Therefore, an exchangeable parameter tuning component is attached to the driving module. Since the parameter tuner and the driving module only need to exchange a convenient performance measure and sets of model parameters, the two components do not need to know anything about each other's implementation allowing a loose coupling and ensuring modularity.

Alternative Control Strategies Model Predictive Control (MPC) has established itself as a popular control strategy. Using a model, the controller can estimate the future state of the robot given a series of inputs. The goal of MPC is to find a series of control inputs minimizing the error predicted using this model. MPC needs to solve an optimization problem in every time step, which makes the approach computationally intense. Further drawbacks are the need for an appropriate model of the process and possible instability (Camacho and Alba, 2013). An alternative control approach being researched which solves instability issues of MPC and other problems is sliding mode control (Utkin, 2009).

Main Controller The goal of a closed-loop controller is to compare the state of the plant, including the vehicle speed and position, measured by the sensors with the desired state and to generate appropriate actuator actions as a reaction to the deviation. In Fig. 7 the graphical C&C model of the *Main Controller* is illustrated and will later serve as a basis for a formal textual model definition in MontiCAR.

For a better readability, only port names and types of the outer component are given in the figure. Note that primitive numeric types are denoted by the allowed range of values and in some cases the unit of the quantity. This high level type system, introduced in (Kusmenko et al., 2017) allows for a more precise modeling than by using conventional primitive types such as integers, floats, and doubles. For instance, it allows to constrain the maximum speed of the vehicle and to specify the measurement accuracy of its sensors. Furthermore, it provides means of compatibility checking specific for the CPS domain. As an example, a speed port cannot be connected to an acceleration port, since the two quantities have different unit types. This feature helps preventing logical errors in the model by appropriate compiler errors. To keep the model compact, primitive types belonging together such as two-dimensional coordinates and PID tuples are grouped into structs.

On the left hand side of the diagram input ports including filtered sensor data as well as PID parameters found by parameter tuner are depicted. Further inputs are track data and the current trajectory goal, i.e., the next target point. The right hand side shows output ports for actuating variables as well as an interface to the genetic algorithm. The `brake`, `steering`, `gear`, and `gasPedal` values are forwarded to the actuator interface via the data adapter whereas the *errors* value is forwarded to the tuner component. The behavior of the main controller block is specified by the interconnection of its subcomponents which are partially taken from a library and partially designed as primitive components for this case study using MontiCAR's math language.

Although the graphical model is well suited to provide a quick comprehensive overview of the system, textual modeling provides several advantages such as easier version control and collaborative editing, searching and comparing the models, and others. An excerpt of the textual MontiCAR model for the controller architecture is illustrated in Fig. 8.

The component is defined using the `component` keyword. It consists of a set of input and output port declarations as well as a set of subcomponents instantiated using the keyword `instance`. Finally components are reconnected with each other in order to define the data flow. Thereby, output ports of a component can only be connected to type compatible input ports. Note that the underlying semantics of MontiCAR is weakly causal, i.e., the computation result of a component is available instantaneously; neither computations nor connectors introduce delays.

Before stepping into the details of how the controller output values are computed, the extract components are explained. These are needed to understand how the parameter tuner communicates with the controller. To optimize the parameter values for the three PID controllers, their parameters need to be passed to the controller as an input. This way, the quality of the parameter sets can be evaluated during the driving process. Each PID controller takes three parameters, the P-term, the I-term, and the D-term, form-

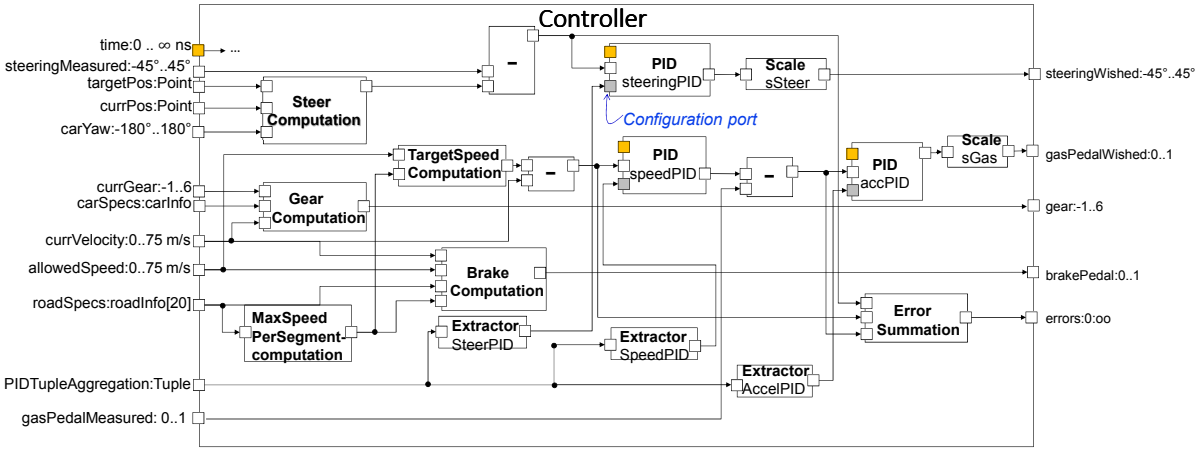

Fig. 7: Main controller component calculating the actuating variables and providing the interface to the genetic algorithm.

```
component Controller{
  ports
       in Q(-45° : 0.001° : 45°) steering,
       in Point targetPoint,
       in Point currPos,
       in Q(-180° : 0.001° : 180°) carYaw,
       /*other input and out ports*/

       instance SteerComputation steerComp;
       instance Subtract subtractSteer;
       instance PID<°> steeringPID(-45°, 45°, 10°);
       connect targetPoint -> steerComp.targetPoint;
       connect currPos -> steerComp.currPos;
       connect carYaw -> steerComp.carYaw;

       connect steerComp.targetSteerAngle ->
                        subtractSteer.targetVal;
       connect steering -> subtractSteer.measuredVal;
       /*Other connectors*/
 }
```

Primitive MontiCAR type consisting of the number type (Q=rational, Z=integer, C=complex), the range and the resolution

Struct type

The components are getting declared with the keyword instance

Instantiation of a parameterized PID with the bounds -45° and 45°

The ports of the components are getting connected via the keyword connect and an arrow „->"

Fig. 8: MontiCAR code describing the graphical controller model of Fig. 7.

```
component PID<U is Unit>                                    EMA
        (Q(-oo U:oo U) lower, Q(-oo U:oo U) upper, Q(0 U:oo U) windup){
  ports in Q(0 s:oo s) time,
         in Q(-oo U : + oo U) error,
         in PIDTuple pid,
         out Q(-oo U :oo U) output;
  implementation Math {
    static Q(0 s:oo s) prev_time = time;
    static Q(-oo U:oo U) prev_error = error;
    static Q(-oo U:oo U) int_error = 0;
    Q(0s:oo s) dT = time - prev_time;
    int_error = int_error + 0.5Hz*dT*(error + prev_error);
    int_error = max(min(windup, int_error), -windup);
    T P_term = pid.P*error;
    T I_term = pid.I*int_error;
    T D_term = 1s * pid.D*(error - prev_error)/dT;
    prev_time = time;
    prev_error = error;
    output = P_term + I_term + D_term;
    output = min(max(lower, output), upper);
} }
```

PID parameters can be updated at any time through the **pid** port (but should only be updated when a lap is finished according to requirement **R9**)

Initialization part of **static** variables takes place only in first execution cycle

Setting bounded value of the output port

Fig. 9: MontiCAR specification of a PID controller with an integral windup guard

ing a parameter tuple. To bundle these three parameter tuples for all three PID controllers, a struct called `PIDTupleAggregation` is used. In addition, this struct contains a fitness value which is used later on by the parameter tuner. The components `Extractor SteerPID`, `Extractor SpeedPID` and *Extractor AccelPID* are used to extract the right PID parameter tuple from the `PIDTupleAggregation` struct before being inputted to the respective PID controller. The controller communicates the following four control variables to the actuator interface: steering angle, brake pedal value, gas pedal value, and the gear. To compute these output values there is a need for several different components. First, the components to calculate the steering angle are outlined.

The `SteerComputation` component takes the target position, the current position, and the current car yaw angle as inputs. By means of these three values the output steering angle is computed according to (Bernhard Wymann and Sumner, 2013). In Fig. 10 the definition of the *SteerComputation* component is depicted. Here a further example of MontiCAR's unusual type system is provided: the car yaw can only take values between -180 and +180 degrees with a resolution of 0.001 degree. The compiler uses this information for component compatibility checks by symbolic execution. If a range violation cannot be detected at compile-time but occurs at runtime, an exception is thrown by the application. Furthermore, the unit declaration makes sure the port input is interpreted as degrees and not as radiants. If the sender provides a radiant based version, an automated conversion takes place. *SteerComputation* is a primitive component, i.e., it does not contain any subcomponents and, hence, requires a behavior description provided here in MontiCAR's Math language. The latter uses the aforementioned type system, as well. Furthermore, it provides standard mathematical functions such as `atan` as well as integrated support for matrix operations.

The current steering angle needs to be subtracted from the target steering angle to get the steering error. The steering error then acts as one input value of a

```
1  component SteerComputation{
2    ports
3        in Point targetPoint,
4        in Point currPos,
5        in Q(-180° : 0.001° : 180°) carYaw,
6        out Q(-45° : 0.001° : 45°) targetSteerAngle;
7    implementation Math{
8      Q(-oo : 0.0001 : oo) targetAngle = atan(targetPoint.y -
             currPos.y, targetpoint.x - currPos.x) - carYaw;}
9      targetSteerangle = targetAngle;
10   }
11 }
```

input values needed for the of the target steering angle

min. value Step size max. value

Setting the output value

Fig. 10: The target steering angle is computed by means of the three input values: `targetPoint`, `currPos` and `carYaw`. In the end the target steering angle is written to the output.

PID controller. The other input for the PID controller is the PID parameter tuple. The PID component is implemented as a parallel structure according to (Åström and Hägglund, 1995). Its specification is formalized using MontiCAR in Fig. 9. Note that the unit of the error to be controlled by the PID may depend on the application. Therefore, the PID component has a generic unit parameter `U` which is a `Unit`. The latter is bound to `JScience javax.measure.unit.Unit` making it compatible with JSR275 (Dautelle and Keil, 2010). In the implementation part, the keyword `static` is introduced. The value of a static MontiCAR variable remains available when an execution cycle is finished. Furthermore, the initialization expression provided with the static variable's definition is only evaluated in the first execution cycle. Dynamic systems such as the PID controller depend not only on the current inputs but also on the past and, hence, can be modeled efficiently using this new language construct while superseding the need of memory blocks.

Since the output of a PID component is theoretically not bounded, we constrain it to have a minimal and a maximal output value of $-45°$ and $45°$, respectively. This is done similar to Simulink by providing additional parameters to the PID in line 9 of Fig. 8.

In order to compute the fitting acceleration and braking, information about the road is required. In TORCS the road is divided into segments. The following properties of the road segments are known and stored in the map data: length, radius, friction coefficient, an *enum* value capturing the segment type (straight or curved), as well as the distance to the segment end to determine where the car is situated in the current segment. The distance to the segment end attribute equals the length of the segment for every segment, except the one the car is currently driving on. These properties are inputted to the controller as a `roadInfo` struct array. The definition of this struct is outlined in Fig. 11.

The acceleration in driving direction is controlled by the gas pedal which takes an input value in

The segment type defines whether the segment is straight or not

```
1 struct roadInfo { Q(0:0.001:50) frictionCoefficient;
2   SegmentType segType;
3   Q(0 m : 0.0001 m : 10 m) length;
4   Q(0 m : 0.0001 m : oo m) radius;
5   Q(0 m : 0.0001 m : 10 m) distToSegEnd;}
```

All relevant attributes of a road segment summarized in a struct

Fig. 11: The struct containing road information about one segment. An array of twenty struct realizations is inputted to the controller in every execution cycle.

the range from zero (no acceleration) to one (maximum acceleration in driving direction) . First of all the maximal speed, the car is able to drive in the foreseeable road segments, is calculated. Thus a maximal speed value for each of these road segments is calculated. These values are needed for the car to stay on track and not lose control in the curves due to a too high velocity. The maximal speed values per segment are computed in the `MaxSpeedPerSegmentComputation` component, by means of the `roadInfo` array. The output will be another array containing the maximal speed value for each segment.

Furthermore the target speed needs to be computed. The `targetSpeedComputation` component takes as input the allowed speed, which can be for example the speed limitation for that road, and the array of the maximum speed values per segment. Additionally, it has a parameter defining how many track segments to consider. By means of these values the target speed is computed. The target speed value is subtracted from the current speed value to get the speed error. This happens in a subtraction component. The speed error is then inputted in a PID component together with the designated PID parameter tuple. By means of these two inputs the PID component calculates the desired acceleration.

The desired acceleration is then subtracted from the current acceleration to compute the acceleration error. It is then inputted along with the designated acceleration parameter tuple into the PID controller. The PID controller, responsible for the regulation of the gas pedal, outputs, by the means of these two inputs, a fitting value for the gas pedal. Since the PID controller does not output bounded gas pedal values, it has to be bounded. Therefore the gas pedal value is inputted in the `GasScale` component which restricts the gas value to the closed interval from zero to one. The bounded value is then forwarded to the gas pedal actuator. With the combination of these two PID controllers, the vehicle is able to adjust its velocity according to a reference value.

The error calculated by each of the subtraction components gets inputted to the `ErrorSummation` component. There the absolute value of each error is calculated before being summed up and outputted

to the parameter tuning component. The latter needs the summation of the error values to measure the performance of the currently used parameter tuples.

Lastly the components used to calculate the appropriate brake pedal value are elucidated. The `Brake-computation` component has four input values: the current velocity, the allowed speed, the road information array, and the maximum speed per segment array. There are two different cases in which the brake value is computed. The first case is given when the allowed speed is lower than the current speed. Then the brake value is computed according to Equation 2:

$$brake = \frac{allowedSpeed - currSpeed}{allowedSpeed}. \quad (2)$$

The second case where braking is needed is when it is assumed that the car is driving on a straight line with the speed v_1. In distance d there is a turn where the allowed speed is v_2 with $v_2 < v_1$. In order to know when to start braking, the minimal braking distance s needs to be computed. The car has a certain amount of kinetic energy which it needs to reduce in order to ride safely through the turn. When braking the car loses kinetic energy. According to the principle of energy conservation, the equation

$$\frac{m \cdot v_1^2}{2} - \frac{m \cdot v_2^2}{2} = m \cdot g \cdot \mu \cdot s[J] \quad (3)$$

can be formed where μ is the friction coefficient, m is the mass of the car and g describes the gravitational acceleration ($9.81 m/s^2$). The equation

$$s = \frac{v_1^2 - v_2^2}{2 \cdot g \cdot \mu}[m] \quad (4)$$

is obtained when solving equation (3) for s.

When the braking distance s is equal or less than the distance d to the curve, the car needs to brake. The braking values are computed according to (Bernhard Wymann and Sumner, 2013).

By means of C&C modeling the developer only has to deal with the homogeneous interface of the data adapter providing access to all sensor signals as well as all possible actuator inputs.

Controller Tuning For the aforementioned tuning of the controller we apply an evolutionary algorithm which is a meta-heuristic optimization inspired by biological evolution processes such as reproduction, selection, recombination, and mutation. Genetic algorithms belong to the family of evolutionary algorithms and are defined by probabilistic selection of the parents and their recombination. The mutation operates more in the background as it only gets executed with a relatively low probability (Weicker, 2007). In this paper an individual is a set of three PID parameter tuples containing the PID values for speed, steer, and acceleration. A set of individuals form a population. The current population produces new individuals that form the new generation. The individuals of the new generation are supposed to have a better average performance than the individuals from the previous generations (Kim et al., 2008).

Fitness function During one lap the errors of steering, speed, and acceleration are measured in each time step. The errors get squared before being multiplied by the time step ΔT. Summing up that expression for every time step, dividing it by the total time T_{total} results in the mean squared error

$$MSE = \frac{1}{T_{total}} \cdot \sum_n \|e(n)\|_2^2 \cdot \Delta T. \quad (5)$$

The fitness function is used to measure the performance of individuals during the process. The higher the fitness value the better the performance of one individual. The fitness function used in this paper is defined as the negative value of the mean squared error:

$$f = -MSE. \quad (6)$$

The duration ΔT of the n-th execution cycle is defined as the difference between t_{n-1} and t_n. T_{total} denotes the total simulated time of one lap. The fitness value is then saved as an attribute in an individual, where it gets evaluated during the evolution process.

Evolution process After the fitness of every individual is evaluated, a new generation is created. The following steps are performed in order to generate a new population:

- Probabilistic parent selection
- Recombination
- Mutation

The first step consists of the probabilistic selection of an appropriate individual based on the fitness value. In this paper the selection is done with tournament selection according to (Weicker, 2007). The tournament selection function picks randomly k individuals of the population and returns the individual with the best fitness.

After selecting the best individuals from the population, the recombination step is executed with a certain probability p. The recombination step recombines two of the selected individuals using arithmetic crossover as prescribed by (Weicker, 2007). With a probability of $(1-p)$ no crossover is performed and one selected individual immediately arrives in the next step. The arithmetic crossover component gets

```
component ArithCrossOver {
  ports in PIDTupleAggregation father,
          PIDTupleAggregation mother,
          Q(0:1) a,          <- Uniformly distributed random variable
       out PIDTupleAggregation tupleOut;
implementation Math {
  PIDTupleAggregation tuples;
  tuples.fitness = 0;
  for i = 1:2
    tuples.tuple[i].P = a*father[i].P + (1-a)*mother[i].P;
    tuples.tuple[i].I = a*father[i].I + (1-a)*mother[i].I;
    tuples.tuple[i].D = a*father[i].D + (1-a)*mother[i].D;
  end
  tupleOut = tuples;
}}
```

Arithmetic crossover, performed on every PID parameter tuple

Fig. 12: Function performing arithmetic crossover for two PIDTupleAggregation structs.

two individuals we refer to as father and mother as input parameters and outputs one individual, the child. By means of a uniformly distributed random variable $\alpha \sim unif(0,1)$ an arithmetic crossover between the two parents is performed. The arithmetic crossover operation is defined as

$$child = \alpha \cdot father + (1-\alpha) \cdot mother. \tag{7}$$

The MontiCAR component performing the crossover is depicted in Fig. 12. To ensure the testability of this component the random variable it relies on is not generated inside the component's implementation part but is provided via an input port. Since MontiCAR semantics is based on the Focus stream theory (Broy and Ştefănescu, 2001; Broy and Stolen, 2012) all output port streams (timed values including history) depend only on input port streams, the mathematical implementation does not contain any dirty not specifiable behavior functions such as random numbers, current system time or any hardware states (all these values must be passed to a component and connector model directly via ports).

In the mutation step the individual gets mutated with a certain probability q. The mutation is performed according to the Gaussian mutation in (Weicker, 2007). The mutation step for one parameter is performed by means of a normally distributed random variable $\beta = \mathcal{N}(\mu, \sigma^2)$ where μ is the mean and σ^2 is the variance of the distribution (Cramer et al., 2008). To each parameter of one individual a normally distributed number is added in order to form the new parameter. Thereby, the mean μ of the normal distribution is the original parameter value.

The mutation step is important in order to keep the genetic diversity intact and thus to be able to find the global optimum. The selection, recombination, and mutation steps are repeated until a new population of the same size as the old population is reached. In Fig. 13 an overview of the genetic algorithm is illustrated.

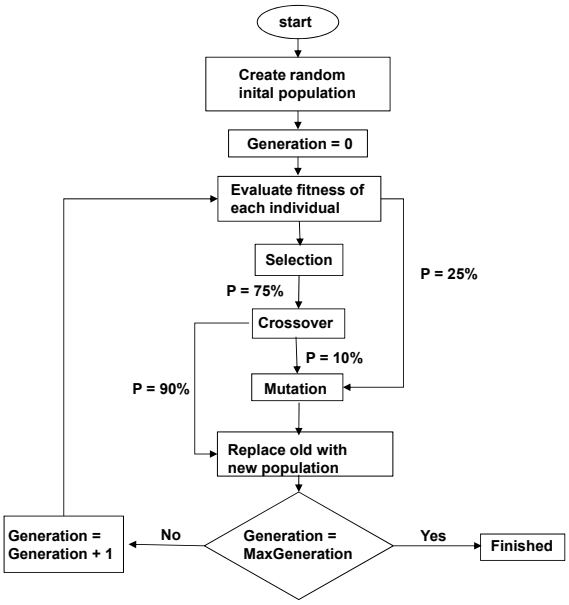

Fig. 13: Genetic Algorithm inspired by (Rathore and Kumar, 2015)

6 DERIVING TESTS FROM C&C MODELS

Based on the SysML internal block diagram model, e.g. the component and connector one shown in Fig. 7, stream specifications mapping input port values to expected output port values can be derived.

Since the main controller component in Fig. 7 is underspecified by containing nine configuration parameters, the three parameters P, I and D for each PID controller instance, the output values for the stream ports are parametrized terms instead of concrete numbers. Fig. 14 shows the generated test stream for one PID controller instance. The parametrized tests are used to check the results of the concrete PID controller generated by the genetic algorithm. These test check whether the P, I, and D parameters are actually positive and that these values do not change during one lap (the same parameter set must be used for $time = 0.1s$ and for $time = 0.5s$).

When concrete output values, after executing the Layer 3B model in the simulator, are present they are compared against the parametrized one by using Microsoft Z3 SMT solver (Barrett et al., 2013; De Moura and Bjørner, 2008). For the parametrized stream in Fig. 14 the mathematical query for the SMT solver is shown in (8).

$$\begin{aligned} P,I,D \in \mathbb{Q}_+ : 10.08° &\geq 3° \cdot P - 0.1° \wedge \\ 10.08° &\leq 3 \cdot P - 0.1° \wedge \\ 131.08° &\geq 4° \cdot P + 0.35° \cdot I + 10° \cdot D - 0.1° \wedge \\ 131.08° &\leq 4° \cdot P + 0.35° \cdot I + 10° \cdot D + 0.1° \wedge \ldots \end{aligned} \tag{8}$$

For the generated C&C model with fixed parameters a stream specification is derived. These stream specifications can be used to verify the functionality of hardware-optimized software for a PID controller running on low-budget and low-energy microcontrollers. Fig. 15 shows an excerpt of an assembler code (Gray, 2004) of a PID controller implemented in Layer 4. Note that the assembler code is over 500 lines while the MontiCAR model in Fig. 9 specifies the PID controller's behavior in about 30 lines. The assembler code for a specific chip can be automatically analyzed for energy consumption and real-time capability requirements, but verifying the functional correctness of the assembler PID controller is very time-consuming. Thanks to the automatically generated tests based on the C&C model specification, functional tests for the assembler code ensuring that the assembler code satisfies its specification are given for free, and additionally, the models of the two layers are always consistent.

7 REQUIREMENTS TESTING OF LAYER 3B

Parameter Tuning Simulation is a common means of model execution and testing. A simulator for MontiCAR models has been proposed in (Grazioli et al., 2017). The following three experiments are conducted in TORCS which is more specialized to our scenario. We choose a track with a width of 15 meters and a length of 2057.56 meters. The physics and the engine simulation is called with a frequency of 500 Hertz whereas the autonomous driving components are called with a frequency of 50 Hertz. The car used is a Chevrolet Corvette T-Top.

```
1  parametrized stream SteeringTest                                    Stream
2   for Controller.steeringPID
                                          Paramaters are not negetive
3   with P in Q+, I in Q+, D in Q+ {
                                  Models on time step
4    time = 0s tick 0.1s tick 0.2s tick 0.3s
5           tick 0.4s tick 0.5s;
6    error = 3° tick 4° tick 2° tick 0° tick -3° tick -1°;
                                  Accuracy: P*3°-0.1° ≤ output ≤ P*3°+0.1°
7    output = P*3° +/- 0.1° tick
8             P*4° + I*0.35° + D*10° +/- 0.1° tick
9             P*2° + I*0.7° - D*35° +/- 0.1°  tick
10            I*0.78° - D*10° +/- 0.1° tick
11            -P*3° + I*0.65° - D*41.67° +/- 0.1° tick
12            -P*1° + I*0.39° + D*72.11° +/- 0.1°;
13 }
```

Fig. 14: Parametrized test stream derived from Component and Connector Model. It uses for simplicity reasons an unbounded PID controller where the output is not limited as in line 20 in Fig. 9. (Integral has been approximated with `integral(@(t) interp1(time, e, t, 'pchip'), 0, t)`, derivation has been approximated with `ppval(fnder(spline(time, e), 1), t))`.

```
137                * ROUTINE TO DO INTEGRAL TERM *
138
139  007F DC00      DOKIT   LDD     ADRCX                   GET CURRENT CONVERSION
140  0081 D300              ADDD    ADRCXM1                 FORM (ADRCX + ADRCXM1)/2
141  0083 04                LSRD
142  0084 DD00              STD     LTEMP2
143  0086 2507              BCS     JMHAPI
144  0088 CC0000            LDD     #$0000
145  008B DD02            STD     LTEMP2+2                FRACTIONAL PART OF FINAL ERROR
```

Fig. 15: Excerpt of Assembler code for PID controller running on MC68HC11K4 microcontroller (Gray, 2004).

In the first experiment the average error of each generation is measured using the genetic algorithm on all three PID tuples. In the second experiment the genetic algorithm is applied in a first stage to train the speed and acceleration PID parameters and in a second stage to train the steering PID parameters. A parameter which is not being optimized is set to a constant value, i.e., during stage one, the steering PID parameters are constant while in the second stage, the acceleration and speed PID parameters are constant. Furthermore the acceleration error and the speed error connections to the `ErrorSummation` component are dropped in the first stage in order to evaluate the steering error in the fitness function only. In the second stage the steering error connection to the `ErrorSummation` component is dropped in order to evaluate the speed and acceleration error in the fitness function only. The error

$$e = x_{target} - x_{measured} \tag{9}$$

is defined as the target value subtracted of the measured value. Thereby x may serve as a placeholder for each controlled variable such as the velocity, acceleration, and the steering angle.

In the third experiment different noise levels are applied to the current position, the target position, the car yaw angle, the gas pedal values, the steering angle, and the current speed in order to understand the noise level our system is able to cope with. The genetic algorithm trains the PID parameters for 5 generations for each noise level before recording the MSE for the best PID parameters.

Training all parameters together To efficiently measure the acceleration error and speed error, the target speed is changed every thirty seconds alternating between ten and seventeen meters per second. This means that every thirty seconds the target speed changes by seven meters per second alternating up and down. To have the same conditions for every individual in the population, the errors of one individual is measured during one whole lap (see Sec. 5). This is extremely important regarding the steering error. If it is not measured under the same circumstances, it may happen that an individual which has a good performance, has a worse fitness value than another parameter set which has a worse performance, but had

an "easier" path. Since the steering error is about two orders of magnitude smaller than the acceleration and the speed error, it gets multiplied by a weight before being inputted to the fitness function. In Fig. 16 (a) the averaged MSE over the generations is illustrated. It can be concluded that the vehicle is able to follow the trajectory at a given speed. Since the course of the plot converges and the MSE is declining, our system fulfills requirement **R3** shown in Fig. 3.

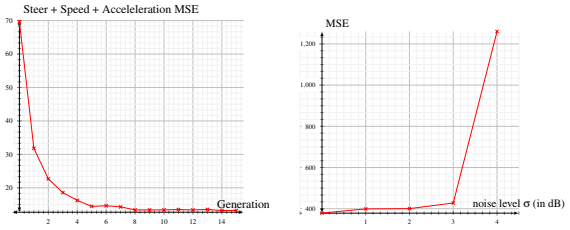

(a) (b)

Fig. 16: In (a) the overall MSE, including steering, acceleration an speed is depicted over the generations 0 to 15. In (b) the MSE of the optimal PID parameters with different noise levels is illustrated.

Training in two sets of parameters This experiment is divided in two stages. In the first stage the acceleration and speed PID parameter tuples are trained. In the second stage the steering PID parameter tuple is trained. In stage one the steering PID parameter tuple needs to be fixed. In order to fix that tuple, the best PID steering tuple of the first experiment is taken. This tuple is then inputted to the PID component which is responsible for the steering. Furthermore the connection between the `Subtraction` component responsible for the steering error and the `ErrorSummation` component are dropped. Thus the steering error will not influence the fitness value. It is also assured that the steering PID tuple does not bias the speed and acceleration due to a poor choice of parameters. To efficiently measure the acceleration and speed error, the target speed is changed every thirty seconds alternating between twenty and thirty meters per second. On the left hand side of Figure 17 the MSE of the speed and acceleration over the generations is illustrated. Note that the absolute values of both experiments cannot be compared due to different underlying meta data.

In the second stage of the experiment only the steering PID parameters are trained. Thus we input constant parameter tuples to the PID controllers responsible for the speed and the acceleration. Furthermore the connections between the two *Subtraction* components and the `ErrorSummation` component is dropped. Thus only the steering error is evaluated by the fitness function. On the right hand of Figure 17,

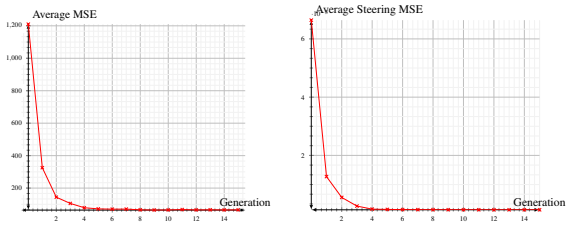

(a) (b)

Fig. 17: In (a) the MSE of the acceleration and speed only is shown. In (b) the MSE of the steering is shown.

the MSE of the steering PID parameter tuple is depicted. In the two stages of the second experiment, it is proved how simple it is to test different setups just by dropping connections and providing different inputs to certain components.

Noise level analysis Other than in the simulator, it is not possible for a sensor to measure certain physical values, e.g. the current position, with infinite accuracy. For acceptance testing we make the application more realistic by modeling sensor imperfections using the Additive White Gaussian Noise (AWGN) model (Cover and Thomas, 2012). Then, a sensor measurement of the ground truth value X_i at time step i is defined as

$$Y_i = X_i + Z_i \tag{10}$$

$$Z_i \sim \mathcal{N}(0, \sigma). \tag{11}$$

Thereby, X_i is a placeholder for any of the measured quantities, namely, speed, gas pedal value, steering angle, yaw angle, the current and the target position. To filter the noisy sensor signals, low-pass filters are used. The experiment is executed for five different noise levels. For each of these noise levels, the PID parameters were trained for five generations. After the training, the MSE of the best PID parameter set for each noise level was measured during one lap with the respective noise levels. After the fifth noise level of 5 dB, the car could not be brought under proper control and crashed, meaning that the maximum admissible noise level was surpassed. In Fig. 16 on the right hand side the MSE with respect to the noise level is depicted. Apparently, the system is able to handle sensor imperfections up to a critical noise level ($\sigma < 3dB$). The latter can be found by means of Fig. 16.

A video of racing car tuning its parameters is available at:
`https://youtu.be/7llpVLklnPY`

8 CONCLUSIONS

In this paper a novel modeling approach for CPS following the SMARDT methodology was evaluated. Therefore, a self-driving vehicle controller for driving on a track in TORCS was developed. Using formal SysML diagrams and the MontiCAR modeling language it was possible to hierarchically design the system and evaluate its performance. Novel language elements such as component and connector arrays proved to enhance component decoupling and reuse, e.g., by allowing the evolutional parameter tuner to connect to arbitrary many PID components. The strong type system supporting units enabled efficient component integrity checks. The modular architecture description enabled the developers to experiment with many different variants and configurations of the system. Thereby, a suitable control strategy could be found and evaluated in an efficient manner. Finally, the models were used to generate a working system. Hence, it was shown that MontiCAR is a homogeneous development framework for modeling, verification, testing, and generation of CPS.

Acknowledgements This research was supported by a Grant from the GIF, the German-Israeli Foundation for Scientific Research and Development, and by the Grant SPP1835 from DFG, the German Research Foundation.

REFERENCES

Accellera SYSTEMS INITIATIVE (2014). Verilog-AMS Language Reference Manual. Technical Report 2.4.0.

Aravantinos, V., Voss, S., Teufl, S., Hölzl, F., and Schätz, B. (2015). AutoFOCUS 3: Tooling Concepts for Seamless, Model-based Development of Embedded Systems. In *ACES-MB*.

Ashenden, P. J. (2010). *The designer's guide to VHDL*, volume 3. Morgan Kaufmann.

Åström, K. J. and Hägglund, T. (1995). *PID controllers: theory, design, and tuning*, volume 2. Isa Research Triangle Park, NC.

Baheti, R. and Gill, H. (2011). Cyber-physical systems. *The impact of control technology*, 12.

Barrett, C., Deters, M., de Moura, L. M., Oliveras, A., and Stump, A. (2013). 6 Years of SMT-COMP. *J. Autom. Reasoning*, 50(3).

Beck, K., Beedle, M., Van Bennekum, A., Cockburn, A., Cunningham, W., Fowler, M., Grenning, J., Highsmith, J., Hunt, A., Jeffries, R., et al. (2001). Manifesto for agile software development.

Berger, C. (2016). An Open Continuous Deployment Infrastructure for a Self-driving Vehicle Ecosystem. In *IFIP International Conference on Open Source Systems*.

Bernhard Wymann, Eric Espié, C. G. C. D. R. C. and Sumner, A. (2013). TORCS, the open racing car simulator.

Bertram, V., Maoz, S., Ringert, J. O., Rumpe, B., and von Wenckstern, M. (2017). Case Study on Structural Views for Component and Connector Models. In *MODELS*.

Bertram, V., Roth, A., Rumpe, B., and von Wenckstern, M. (2016). Extendable Toolchain for Automatic Compatibility Checks. In *OCL'16*.

Bojarski, M., Del Testa, D., Dworakowski, D., Firner, B., Flepp, B., Goyal, P., Jackel, L. D., Monfort, M., Muller, U., Zhang, J., et al. (2016). End to end learning for self-driving cars. Technical report, NVIDIA.

Bröhl, A.-P. and Dröschel, W. (1995). Das V-Modell. *München, Wien: Oldenburg-Verlag*.

Broy, M. and Rausch, A. (2005). Das neue v-modell® xt. *Informatik-Spektrum*, 28(3).

Broy, M. and Ştefănescu, G. (2001). The algebra of stream processing functions. *Theoretical Computer Science*, 258(1-2).

Broy, M. and Stolen, K. (2012). *Specification and development of interactive systems: focus on streams, interfaces, and refinement*. Springer Science & Business Media.

Camacho, E. F. and Alba, C. B. (2013). *Model predictive control*. Springer Science & Business Media.

Chen, C., Seff, A., Kornhauser, A., and Xiao, J. (2015). Deepdriving: Learning affordance for direct perception in autonomous driving.

Cover, T. M. and Thomas, J. A. (2012). *Elements of information theory*. John Wiley & Sons.

Cramer, E., Kamps, U., and Steland, A. (2008). *Grundlagen der Wahrscheinlichkeitsrechnung und Statistik*. Springer.

Dautelle, J.-M. and Keil, W. (2010). JSR 275: Units Specification. Java specification request, RWTH Aachen.

De Moura, L. and Bjørner, N. (2008). Z3: An efficient SMT solver. In *TACAS*.

Dormoy, F.-X. (2008). Scade 6: a model based solution for safety critical software development. In *ERTS*.

Elmqvist, H., Mattsson, S. E., and Otter, M. (1999). Modelica-a language for physical system modeling, visualization and interaction. In *CAV*.

Friedrich, J., Kuhrmann, M., Sihling, M., and Hammerschall, U. (2009). *Das v-modell xt*. Springer.

Gogolla, M., Büttner, F., and Richters, M. (2007). USE: A UML-based specification environment for validating UML and OCL. *Science of Computer Programming*, 69(1).

Gray, J. W. (2004). PID Routines for MC68HC11K4 and MC68HC11N4 Microcontrollers.

Grazioli, F., Kusmenko, E., Roth, A., Rumpe, B., and von Wenckstern, M. (2017). Simulation Framework for Executing Component and Connector Models of Self-Driving Vehicles. In *EXE at MODELS*.

Grimm, K. (2003). Software Technology in an Automotive Company: Major Challenges. In *ICSE*.

Harel, D. and Rumpe, B. (2004). Meaningful Modeling: What's the Semantics of "Semantics"? *IEEE Computer*, 37(10).

Kim, J.-S., Kim, J.-H., Park, J.-M., Park, S.-M., Choe, W.-Y., and Heo, H. (2008). Auto tuning PID controller based on improved genetic algorithm for reverse osmosis plant. *World Academy of Science, Engineering and Technology*, 47(2).

Kusmenko, E., Roth, A., Rumpe, B., and von Wenckstern, M. (2017). Modeling Architectures of Cyber-Physical Systems. In *ECMFA*.

Liang, Y.-z. D. C., Wang, Y.-z., and Liu, Y.-f. (2004). The formal semantics of an UML activity diagram. *Journal of Shanghai University (English Edition)*.

Liggesmeyer, P. (2009). *Software-Qualität: Testen, Analysieren und Verifizieren von Software*. Springer Science & Business Media.

Maoz, S., Mehlan, F., Ringert, J. O., Rumpe, B., and von Wenckstern, M. (2017). Ocl framework to verify extra-functional properties in component and connector models. In *ModComp at MODELS*.

Maoz, S., Ringert, J. O., and Rumpe, B. (2011). An Operational Semantics for Activity Diagrams using SMV. Technical report, RWTH Aachen.

Mathworks Inc. (2016). Simulink User's Guide. Technical Report R2016b, MATLAB & SIMULINK.

Matinnejad, R., Nejati, S., and Briand, L. C. (2017). Automated testing of hybrid Simulink/Stateflow controllers: industrial case studies. In *FSE*.

Mingsong, C., Xiaokang, Q., and Xuandong, L. (2006). Automatic test case generation for UML activity diagrams. In *AST*.

Modelica Association (2005). Modelica language specification. *Linköping, Sweden*.

Montemerlo, M., Becker, J., Bhat, S., Dahlkamp, H., Dolgov, D., Ettinger, S., Haehnel, D., Hilden, T., Hoffmann, G., Huhnke, B., et al. (2008). Junior: The stanford entry in the urban challenge. *Journal of field Robotics*, 25(9).

National Instruments (1998). BridgeView and LabView: G Programming Reference Manual. Technical Report 321296B-01.

OMG (2015). OMG Systems Modeling Language (OMG SysML). Technical Report Version 1.4.

Palmisano, A., Hoops, S., Watson, L. T., Jones, T. C., Tyson, J. J., and Shaffer, C. A. (2015). JigCell Run Manager (JC-RM): a tool for managing large sets of biochemical model parametrizations. *BMC Systems Biology*, 9(1).

Philipps, J., Pretschner, A., Slotosch, O., Aiglstorfer, E., Kriebel, S., and Scholl, K. (2003). Model-Based Test Case Generation for Smart Cards. *Electronic Notes in Theoretical Computer Science*, 80(Supplement C).

Pretschner, A., Slotosch, O., Aiglstorfer, E., and Kriebel, S. (2004). Model-based testing for real. *International Journal on Software Tools for Technology Transfer*, 5(2-3).

Rathore, A. and Kumar, M. (2015). Robust Steering Control of Autonomous Underwater Vehicle: based on PID Tuning Evolutionary Optimization Technique. *International Journal of Computer Applications*.

Richenhagen, J., Rumpe, B., Schloßer, A., Schulze, C., Thissen, K., and von Wenckstern, M. (2016). Test-driven Semantical Similarity Analysis for Software Product Line Extraction. In *SPLC*.

Rumpe, B. (1996). *Formale Methodik des Entwurfs verteilter objektorientierter Systeme*. Herbert Utz Verlag Wissenschaft.

Rumpe, B. (2003). Model-Based Testing of Object-Oriented Systems. In *Symposium on Formal Methods for Components and Objects*.

Rumpe, B. (2016). *Modeling with UML: Language, Concepts, Methods*. Springer International.

Rumpe, B. (2017). *Agile Modeling with UML: Code Generation, Testing, Refactoring*. Springer International.

Rumpe, B., Schulze, C., von Wenckstern, M., Ringert, J. O., and Manhart, P. (2015). Behavioral Compatibility of Simulink Models for Product Line Maintenance and Evolution. In *SPLC*.

Slicker, J. M. and Loh, R. N. (1996). Design of robust vehicle launch control system. *IEEE transactions on control systems technology*, 4(4).

The Institute of Electrical and Electronics Engineers (1988). Standard VHDL language reference manual. *IEEE Std*.

Urmson, C. et al. (2008). Self-driving cars and the urban challenge. *IEEE Intelligent Systems*, 23(2).

Utkin, V. (2009). Sliding mode control. *CONTROL SYSTEMS, ROBOTICS AND AUTOMATION–Volume XIII: Nonlinear, Distributed, and Time Delay Systems-II*.

V-Modell XT (2006). Part 1: Fundamentals of the V-Modell. Technical report, Federal Government of Germany.

Wei, J., Snider, J. M., Kim, J., Dolan, J. M., Rajkumar, R., and Litkouhi, B. (2013). Towards a viable autonomous driving research platform. In *Intelligent Vehicles Symposium (IV), 2013 IEEE*.

Weicker, K. (2007). *Evolutionäre Algorithmen*. Leitfäden der Informatik. Vieweg+Teubner Verlag.

Ziegler, J., Bender, P., Schreiber, M., and more (2014). Making Bertha Drive; An Autonomous Journey on a Historic Route. *IEEE Intelligent Transportation Systems Magazine*, 6(2).